The Ionized Methylene Transfer from the Distonic Radical Cation $^{+}CH_2—O—CH_2^{\cdot}$ to Heterocyclic Compounds. A Pentaquadrupole Mass Spectrometric Study

Fabio Cesar Gozzo and Marcos N. Eberlin

State University of Campinas, UNICAMP, Institute of Chemistry, CP 6154 Campinas, SP 13081-970 Brazil

Ion–molecule reactions of the mass-selected distonic radical cation $^{+}CH_2 — O — CH_2^{\cdot}$ (**1**) with several heterocyclic compounds have been investigated by multiple stage mass spectrometric experiments performed in a pentaquadrupole mass spectrometer. Reactions with pyridine, 2-, 3-, and 4-ethyl, 2-methoxy, and 2-*n*-propyl pyridine occur mainly by transfer of $CH_2^{+\cdot}$ to the nitrogen, which yields distonic *N*-methylene-pyridinium radical cations. The MS^3 spectra of these products display very characteristic collision-induced dissociation chemistry, which is greatly affected by the position of the substituent in the pyridine ring. Ortho isomers undergo a δ-cleavage cyclization process induced by the free-radical character of the *N*-methylene group that yields bicyclic pyridinium cations. On the other hand, extensive $CH_2^{+\cdot}$ transfer followed by rapid hydrogen atom loss, that is, a net CH^+ transfer, occurs not to the heteroatoms, but to the aromatic ring of furan, thiophene, pyrrole, and *N*-methyl pyrrole. The reaction proceeds through five- to six-membered ring expansion, which yields the pyrilium, thiapyrilium, *N*-protonated, and *N*-methylated pyridine cations, respectively, as indicated by MS^3 scans. Ion **1** fails to transfer $CH_2^{+\cdot}$ to tetrahydrofuran, whereas a new α-distonic sulfur ion is formed in reactions with tetrahydrothiophene. Unstable *N*-methylene distonic ions, likely formed by transfer of $CH_2^{+\cdot}$ to the nitrogen of piperidine and pyrrolidine, undergo rapid fragmentation by loss of the α-NH hydrogen to yield closed-shell immonium cations. The most thermodynamically favorable products are formed in these reactions, as estimated by ab initio calculations at the MP2/6-31G(*d,p*)//6-31G(*d,p*) + ZPE level of theory. *(J Am Soc Mass Spectrom 1995, 6, 554–563)*

Distonic radical cations [1] are fascinating bidentate reagents that usually display a rich reactivity driven by either or both the radical and charge sites, which are formally located at different atoms. In contrast to their neutral counterparts, that is, diradicals or zwitterionic molecules, distonic ions often represent stable and easily accessible gas phase species [2]. Quite surprisingly, these ions are also, in many cases, more stable than isomeric conventional radical cations, a result predicted by theory [3] and confirmed by experimental observations [2]. Although distonic ions usually have no stable counterparts, their gas phase generation often can be accomplished by means of unimolecular fragmentation or isomerization of conventional radical cations. Ion–molecule reactions also have been demonstrated as a very useful approach for gas phase generation of many distonic ions [2]. The chemistry of the stable distonic ions generated by these methods can be studied conveniently in the gas phase by employing multiple stage mass spectrometric techniques [4].

The gas phase chemistry of the distonic radical cation $^{+}CH_2—O—CH_2^{\cdot}$ (**1**), the corresponding ionized form of the simplest, yet unknown, carbonyl ylide $CH_2{=}O^{+}—CH_2^{-}$, has been extensively investigated [2]. Ion **1** has been represented as either $^{+}CH_2—O—CH_2^{\cdot}$ or $CH_2{=}O^{+}—CH_2^{\cdot}$. Considering, however, that both the charge and spin densities are evenly distributed by the two methylene groups, as shown by ab initio calculations [MP2/6-31G(*d,p*)//6-31G(*d,p*)] (see below), one may suggest (a) as the best representation for ion **1**. For simplicity, however, ion **1** will be represented as $^{+}CH_2—O—CH_2^{\cdot}$, the resonance structure that best represents the charge and spin distributions and that emphasizes its distonic character.

Address reprint requests to Dr. Marcos N. Eberlin, State University of Campinas, UNICAMP, Institute of Chemistry, CP 6154 Campinas, SP 13081-970 Brazil.

© 1995 American Society for Mass Spectrometry
1044–0305/95/$9.50
SSDI 1044-0305(95)00246-A

Received November 15, 1994
Revised March 14, 1995
Accepted March 21, 1995

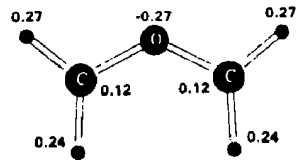

Muliken total charge

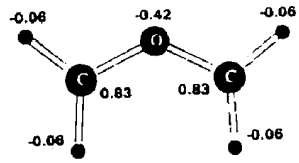

Spin density

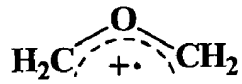

(a)

The distonic, nonconventional ionic structure of $^{+}CH_2—O—CH_2^{\cdot}$ has been well established by several techniques [5], which include its peculiar ion–molecule reactivity [6]. Abstraction of $^{\cdot}SCH_3$ from dimethyl disulfide (and $^{\cdot}SeCH_3$ from dimethyl selenide) followed by formaldehyde loss [5h] and methylene abstraction from ketene [5i] have definitely proven its distonic character [5h]. The most characteristic ion–molecule reaction of ion **1** is net $CH_2^{+\cdot}$ transfer that leads to formation of new distonic ions in several cases. This ion also has been observed recently to display a rich gas phase chemistry that includes a net $C_2H_3O^+$ transfer to benzene and anisole and an ionic 1,3-dipolar cycloaddition reaction with several ketones [7].

In this study, for the first time, a pentaquadrupole mass spectrometer has been applied to explore the gas phase chemistry of a distonic ion. In this multiple stage mass spectrometer, ion–molecule reactions of mass-selected ions can be performed efficiently, and can be followed by product ion mass selection and characterization by further collision-induced dissociation (CID) or ion–molecule reactions. Multiple collision conditions and low collision energies (0–2 eV) are normally applied for ion–molecule reactions in this and other multiple quadrupole instruments [4]. This helps to stabilize the product ions through collisional relaxation or collisional "cooling," which thus allows their observation or the increase of their relative abundances. The usefulness of the pentaquadrupole for detailed gas phase ion–molecule reaction studies recently has been demonstrated in a series of papers [8]. Thus, the ion–molecule reactions of the mass-selected ion **1** with several heterocyclic compounds have been investigated in this study by MS^2 experiments performed in the pentaquadrupole instrument [9], whereas MS^3 scans are applied for product ion characterization. The results enable the proposal of reaction mechanisms and show several applications of these reactions to the synthesis of ionic species and for isomer distinction. Ab initio calculations at the MP2/6-31G(d,p)//6-31G(d,p) + ZPE level of theory were performed on most conceivable ion–molecule reaction products and helped us to understand interesting differences in reactivity that were observed.

Experimental

The experiments were performed via an Extrel (Pittsburgh, PA) pentaquadrupole mass spectrometer that consists of three mass analyzing (Q1, Q3, Q5) and two reaction quadrupoles (Q2, Q4). Ion–molecule reactions or CID were performed by MS^2 experiments in which the first scanning quadrupole (Q1) was used to mass-select the reactant ion generated in the ion source. Ion–molecule reactions were performed with the neutral reagent introduced into Q2 at near 0-eV collision energy, whereas CID employed 10-eV collisions with argon. The corresponding product spectrum was acquired by scanning Q5, while operating Q3 in the nonanalyzing rf-only mode. The collision energies were calculated as the voltage difference between the ion source and the reaction quadrupole. For the MS^3 experiments, one of the ion–molecule products generated in Q2 was mass-selected in Q3 and 10-eV collisions with argon were performed in Q4, while scanning Q5 to record the spectrum. The total pressures inside each differentially pumped region, which correspond to multiple collision conditions in both Q2 and Q4, were typically 2×10^{-6} (ion source), 8×10^{-5} (Q2), and 6×10^{-5} (Q4) torr, respectively.

Ion **1** was generated by dissociative 70-eV electron-impact (EI) ionization of 1,3-dioxolane [5c]. Ion **4a** was obtained by collision dissociation of protonated 3-ethyl pyridine, which was formed in the ion source by methane chemical ionization (CI) of the neutral 3-ethyl pyridine. After selection of the protonated 3-ethyl pyridine in Q1, methyl radical loss that yields **4a** was induced by collisions with argon in Q2. The low energy CID spectrum of **4a** was obtained by a MS^3 scan in which this ion was mass-selected in Q3 and subjected to CID in Q4. The pyrilium (**10a**) and thiapyrilium (**10b**) cations were generated by 70-eV EI of 2-methyl furan and 2-methyl thiophene, respectively [10]. Protonated pyridine (**10c**) and the *N*-methyl pyridinium cation (**10d**) were generated by methane and CH_3I chemical ionization (CI) of pyridine, respectively. The radical cations **12** and **13** were generated by 70-eV electron-impact (EI) ionization of their corresponding neutral molecules.

Ab initio molecular orbital calculations were carried out by using the Gaussian92 program [11]. The ions were optimized at the unrestricted Hartree–Fock (UHF) level of theory by employing the polarization 6-31G(d,p) basis set [12]. Improved energies were obtained by using single point calculations at the 6-31G(d,p) level of theory and by incorporating valence electron correlations calculated by second-order Møller–Plesset (MP2) perturbation theory [13]. Harmonic vibrational frequencies were calculated at the UHF/6-31G(d,p) level to characterize the stationary

points and to obtain the zero-point vibrational energies (ZPE). The input and output structures were visualized with the aid of the Xmol program [14].

Results and Discussion

Reactions with Pyridines

Pyridine. Bouma, MacLeod, and Radom [5d] performed ion–molecule reactions under chemical ionization conditions and have shown that the C—C ring-opened oxirane radical cation, that is, ion **1** [3f] reacts with pyridine to yield predominantly protonated pyridine and a $CH_2^{+\cdot}$ transfer product to a moderate extent. High energy CID and isotopic labeling experiments performed by de Koster, van Houte, and van Thuijl [5f] and by Yu, Gross, and Fountain [5j] have demonstrated that the $CH_2^{+\cdot}$ transfer occurs to the nitrogen and yields the distonic *N*-methylene pyridinium radical cation **2a** (Scheme I).

In this present study, ion **1** was generated in the ion source, mass-selected by Q1, and reacted with pyridine added to the first collision cell (Q2) of the pentaquadrupole instrument. (No changes in the set of products for all the ion–molecule reactions performed in this study were observed when the pressure of the reactant neutral gas was varied considerably, which indicates that the products are formed by primary reactions; that is, they arise mainly from the Q1 mass-selected ion **1**. Collisional cooling of ion **1** with CS_2 in Q2 and further reaction with several reagents in Q4 did not affect significantly the product spectra, which indicate no or negligible ion internal energy effects in this study.) The resultant MS^2 product spectrum (Table 1) shows an abundant $CH_2^{+\cdot}$ transfer product (m/z 93, 100%), which vastly predominates protonated pyridine (m/z 80, 30%). The much greater abundance of the $CH_2^{+\cdot}$ transfer product in the MS^2 experiment when compared to the CI results is most likely

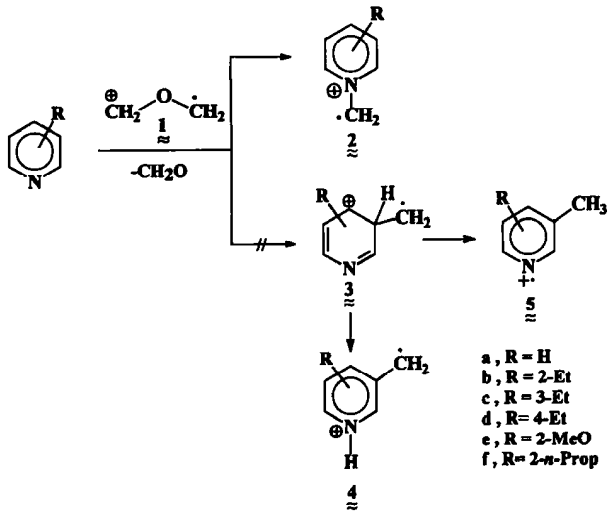

Scheme I

the effect of both the use of the mass-selected ion and of the collisional relaxation of the reaction product proportioned by the low energy multiple collision conditions employed. The collisional stabilization of reaction products under the present experimental conditions becomes evident, for instance, when an abundant adduct is observed for the reaction of ionized pyridine and ethylene (Sorrilha, A. E. P. M.; Pimpim, R. S.; Eberlin, M. N., to appear) and when this result is compared to those obtained by Gross and co-workers [15] under low and high pressure Fourier transform mass spectrometry conditions.

To investigate if low energy CID also is able to distinguish the *N*-methylene pyridinium ion **2a**, the MS^3 sequential product spectrum of the $CH_2^{+\cdot}$ transfer product to pyridine was acquired and compared to the CID spectra of its isomers **4a**, **5a** (Scheme I), ionized 2-methyl, and 4-methyl pyridine (Table 2). The results show that indeed low energy CID can be applied with success to characterize **2a**. The hydrogen atom loss fragment (m/z 92, 2%) is of very low abundance in the spectrum of **2a**, whereas this is a major fragment for all other isomers. Note that a hydrogen atom loss cannot be rationalized easily for **2a** due to the lack of α-hydrogens with respect to the methylene radical site. Also characteristic for **2a** is the relatively high abundance of the m/z 66 fragment when compared to that of the m/z 65 and 67 fragments.

Previous semiempirical calculations [5f,5j] have shown that **2a** is the most thermodynamically favorable product for this reaction. The present higher level ab initio calculations (Table 3) entirely confirm the exactness of the semiempirical predictions.

Ethyl pyridines. The MS^2 product spectra for reaction between **1** and the three isomeric ethyl pyridines are shown in Figure 1. Great predominance of the $CH_2^{+\cdot}$ transfer products (m/z 121) is observed in all three spectra; the protonated pyridines (m/z 108) represent minor products. The other observed peaks are fragments of the $CH_2^{+\cdot}$ transfer products, as confirmed by MS^3 experiments and rationalized in subsequent text, and their presence and relative abundances impart remarkable contrasts to all three spectra.

The MS^2 spectrum of 2-ethyl pyridine (Figure 1a) is exceptionally distinctive because it displays a very abundant (100%) net CH^+ transfer product at m/z 120. This singular reactivity for the 2-ethyl isomer can be rationalized by a process that involves $CH_2^{+\cdot}$ transfer to the pyridine nitrogen to yield **2b** followed by ready loss of a hydrogen atom. This loss can be driven by the free-radical character of the *N*-methylene group in an ortho effect that may operate by (a) a cyclization process that occurs through a δ-cleavage with respect to the methylene radical group or (b) by a [1,5-H] shift followed by α-cleavage (Scheme II). Loss of an α-hydrogen from the 2-ethyl group also could occur through odd spin delocalization over the ring (pathway c in Scheme II), but this process does not appear so likely if

Table 1. MS^2 product spectra of ion–molecule reactions between mass-selected ion **1** and several neutral reagents[a]

Neutral reagent	Product m/z (relative abundance)				
	Ionized reagent	Protonated reagent	CH^+ transfer	$CH_2^{+\cdot}$ transfer	Fragments of the ion–molecule products
Pyridine	none	80(30), 159(3)[b]	none	93(100)	none
2-Methoxy pyridine	109(6)	110(100)	122(34)	123(22)	93(19), 94(43), 108(45)
Furan	68(18)	69(8)	81(100)	82(26)	none
Thiophene	84(4)	85(9)	97(100)	98(12)	none
N-Methyl pyrrole	81(16)	82(6)	94(100)	none	124(2)
Tetrahydrofuran	72(1)	73(12), 145(11)[b]	none	none	71(100)
Pyrrolidine	85(2)	86(100)	97(16)	none	70(8)
Piperidine	71(1)	72(100)	84(38)	none	none

[a] The relative abundance of the reagent ion (m/z 44) is not reported. Some spectra are shown as figures; see text.
[b] The proton-bound dimer.

Table 2. Low energy CID spectra of isomeric conventional and distonic $Py\text{-}CH_2,H^{+\cdot}$ ions

Precursor ion	Relative abundance (%) of CID fragments (m/z)				
	92	78	67	66	65
2a[a]	2	4	17	100	16
4a[a]	100	2	88	84	43
5a (Ionized 3-methyl pyridine)	93	5	95	100	29
Ionized 2-methyl pyridine	42	36	29	100	35
Ionized 4-methyl pyridine	99	2	32	100	24

[a] Obtained by a MS^3 scan; see text.

Table 3. Total, ZPE, and relative energies from structure optimization ab initio calculations

	PMP2/6-31G(*d*, *p*)//6-31G(*d*, *p*) (hartree)	ZPE[a] (kcal/mol)	Relative[b] (kcal/mol)
2a	−286.41867	68.0	zero
3a	−286.31588	66.9	63.3
4a	−286.40632	69.0	8.8
5a	−286.37654	68.1	26.5
7a	−268.12637	55.7	37.8
8a	−268.18861	57.0	zero
7c	−248.35030	65.2	26.0
8c	−248.39106	64.8	zero
11	−593.21247	82.8	19.7
12	−593.23632	84.9	6.7
13	−593.24621	84.3	zero

[a] ZPE energies were scaled by 0.89 to account for the systematic overestimation of the vibrational frequencies by Hartree–Fock calculations; see Pople, J. A.; Schlegel, H. B.; Krishnan, R.; Defrees, D. J.; Binkley, J. S.; Frisch, M. J.; Whiteside, R. A.; Hount, R. F.; Hehre, W. J. *Int. J. Quantum Chem.* **1981**, *15*, 269.
[b] Including ZPE.

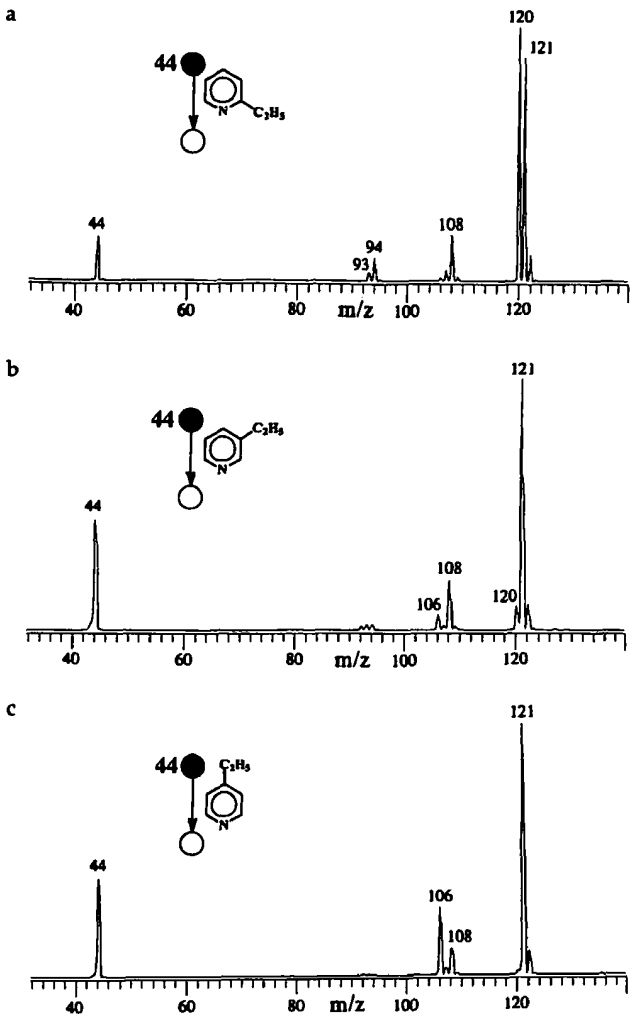

Figure 1. MS^2 product spectra for ion–molecule reactions between the mass-selected ion 1 and (a) 2-ethyl, (b) 3-ethyl, and (c) 4-ethyl pyridine that show the $CH_2^{+\cdot}$ transfer products at m/z 121 and some very characteristic fragments. A filled circle represents a fixed (or selected) mass; an open circle, a variable (or scanned) mass, whereas the neutral reagent or collision gas that causes the mass transitions is shown between the circles. For more details on this nomenclature, see Schwartz, J. C.; Wade, A. P.; Enke, C. G.; Cooks, R. G. *Anal. Chem.* **1990**, *62*, 1809.

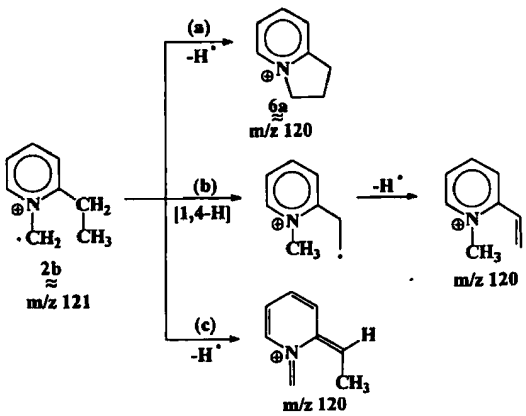

Scheme II

one considers that the CID spectra [15] of all three ionized ethyl pyridines show loss of a hydrogen atom to a great extent, whereas this process occurs here largely and almost exclusively for the ortho isomer. In addition, the ab initio calculations show that the odd spin density is highly localized on the *N*-methylene group (0.90), which should not favor pathway c. These facts are taken, therefore, as indications for the operation of an ortho effect, which has been substantiated by additional experiments, as described in subsequent text. A point in favor of both pathways a and b is that the aromaticity of the pyridine ring is preserved in these processes.

A very special fragmentation also is observed for the para isomer **2d** (m/z 121). This ion shows an abundant fragment at m/z 106 (Figure 1c) that corresponds to loss of a methyl radical. Such fragmentation now can be favored by the relative positions of the ethyl group and the *N*-methylene radical site (Scheme III), which can be classified as a para effect. The fact that the ortho isomer **2b** does not lose a methyl radical appears therefore to indicate that this fragmentation process for **2b** is considerably more energy demanding than that of hydrogen atom loss that occurs through δ-cleavage (Scheme II, pathway a). For **2d**, however, similar δ-cleavage is not possible and methyl radical loss occurs extensively. The para and ortho effects just discussed evidently cannot operate for ion **2c** (the meta isomer); thus neither hydrogen atom nor methyl radical loss is expected to be specially favorable in this case. In agreement with this, ion **2c** shows much greater stability toward dissociation (Figure 1b).

The three MS^3 spectra of the mass-selected isomeric distonic ions **2b–d** (m/z 121) are also very characteristic (Figure 2), which strongly supports their distonic structures and their dissociation pathways affected by the operation of the ortho and para effects, as just discussed.

2-Methoxy and 2-n-propyl pyridine. To investigate by which mechanism (a or b, Scheme II) the ortho effect operates, the reactions of ion **1** with 2-methoxy and

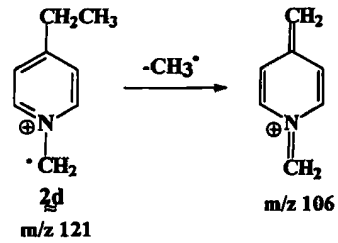

Scheme III

2-*n*-propyl pyridine were examined. Ion **1** reacts extensively with 2-methoxy pyridine by $CH_2^{+\cdot}$ transfer (Table 1); the corresponding product is observed as an abundant peak at m/z 123 (**2e**). This distonic ion, **2e**, similarly to **2b** (Figure 1a), undergoes extensive hydrogen atom loss under the ion–molecule conditions to form m/z 122. Also observed as major products are the ions at m/z 108, 94, and 93 (Table 1). The MS^3 spectrum of **2e** (Table 4) confirms that these product ions, that is, m/z 122, 108, 94, and 93, are fragments of

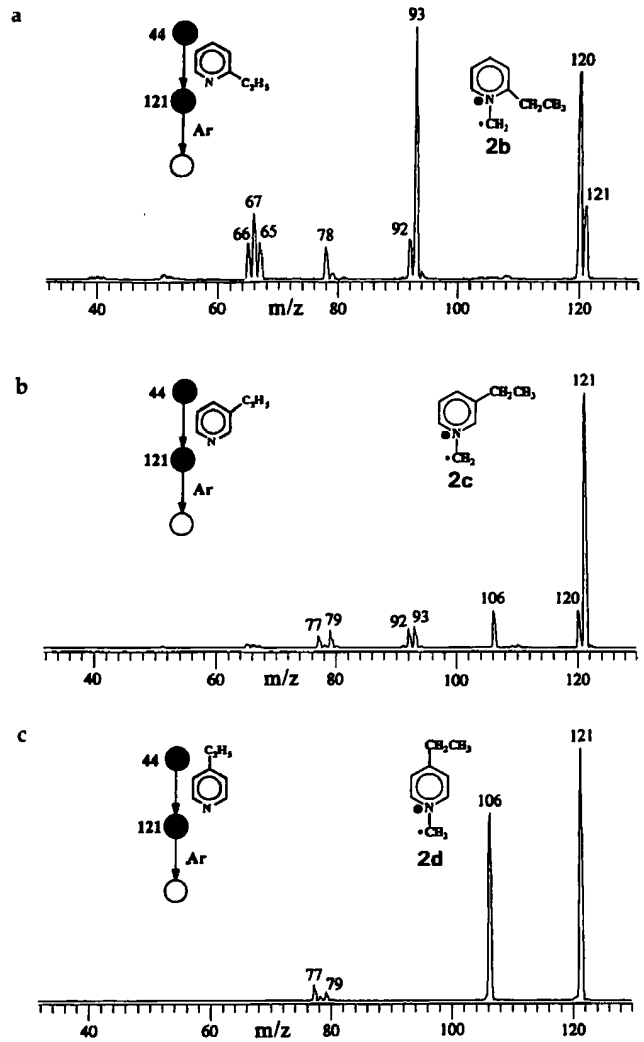

Figure 2. MS^3 sequential product spectra of the $CH_2^{+\cdot}$ transfer products (a) **2b**, (b) **2c**, and (c) **2d** that show in all cases a very characteristic CID fragmentation.

Table 4. MS^3 sequential product spectra of products of ion–molecule reactions between mass-selected ion **1** and several neutral reagents[a]

Neutral reagent	Q3 Selected ion (m/z)	CID products m/z (relative abundance)[b]
2-Ethyl pyridine	120	120(100), 93(9), 92(85), 80(3), 79(6), 78(57), 77(10), 65(43)
2-Methoxy pyridine	123	123(92), 122(11), 108(100), 106(4), 95(3), 94(15), 93(13), 80(15), 78(19)
	122	122(100), 94(23), 93(12), 92(8), 78(7), 67(3), 65(2), 53(4)
2-*n*-propyl pyridine	120	120(100), 93(8), 92(79), 80(3), 79(6), 78(61), 77(11), 65(40)
Furan	81[c]	81(100), 53(41), 51(2), 29(1), 27(12)
Thiophene	97[c]	97(100), 71(1), 69(3), 53(48), 45(26)
N-Methyl pyrrole	94[c]	94(100), 80(1), 79(7), 78(9), 67(6), 65(3), 53(6), 52(3), 51(2), 50(1), 42(1), 41(1), 39(1)
Pyrrolidine	84	84(100), 56(30), 55(13), 42(23), 30(5), 29(2), 28(3)
Piperidine	98	98(100), 70(3), 69(2), 55(14), 44(2), 42(12), 41(13)

[a] The MS^3 spectrum of some products are shown in Table 2 or as figures; see text.
[b] The relative abundance of the selected ion that survives under the CID conditions is also included.
[c] These spectra are nearly identical to the MS^2 spectra of the corresponding ions **10a** (furan), **10b** (thiophene), and **10d** (*N*-methyl pyrrole). For details on the generation of these reference ions, see the Experimental section.

2e. In regard to the operation of the ortho effect, the favorable loss of a hydrogen atom from **2e** (m/z 122) most likely involves its Cβ-H (the 2-methoxy substituent has no Cα-H) in an intramolecular cyclization process (Scheme IV) similar to that proposed in pathway a of Scheme II. By this δ-cleavage mechanism, the bicyclic pyridinium cation **6b** would be formed. It is interesting to note that the δ-cleavages proposed for **2b** and **2e** are analogous to cleavages that have been proposed for ionized 3-(2-pyridyl)-1-propanols, -propyl acetates, -propyl tosylates, and 2-*n*-butyl pyridine *N*-oxide, respectively [16]. In these cases, the δ-cleavages are induced by the ring-nitrogen radical site of the ionized ortho-substituted pyridines and by the oxygen radical site of ionized pyridine *N*-oxide, and analogous bicyclic pyridinium cations are formed.

The ortho effect plays also a key role in the nature of the products of the reaction between **1** and 2-*n*-propyl pyridine (Figure 3). The major product (m/z 120) is most likely the fragment produced by rapid methyl radical loss from the unstable $CH_2^{+\cdot}$ transfer product **2f** (Scheme V). The *n*-propyl side chain of **2f** also drives fragmentation by loss of C_2H_4 to yield the fragment at m/z 107 (Scheme V). Note that fragmentation by loss of a methyl radical can be rationalized best to occur for **2f** by the δ-cleavage process shown in Scheme V, which is again similar to that proposed for **2b** in pathway a of Scheme II. Note also that both processes are expected to yield the same bicyclic pyridinium cation **6a**. On the other hand, pathways similar to b and c should in this case still lead to hydrogen atom or ethyl radical loss, not to the observed methyl radical loss.

A strong indication for the operation of the δ-cleavage process is provided by the MS^3 spectra of the m/z 120 ions formed from both 2-ethyl pyridine and 2-*n*-propyl pyridine (Table 4). The great similarity observed for these two spectra confirms formation of the same bicyclic pyridinium cation **6a** and thus the operation of a similar δ-cleavage in both cases. Note also the characteristic fragmentation by loss of C_2H_4 (m/z 92) and C_3H_6 (m/z 78) displayed for **6a** (Table 4), which can be rationalized to occur at the five-membered saturated ring. Comparable fragmentation by C_2H_4 (m/z 94) and C_2H_4O (m/z 78) loss also is observed for **6b**, the m/z 122 product of 2-methoxy pyridine (Table 4).

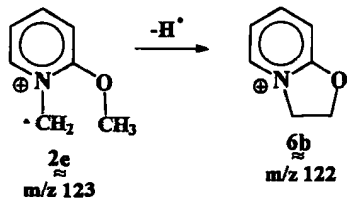

Scheme IV

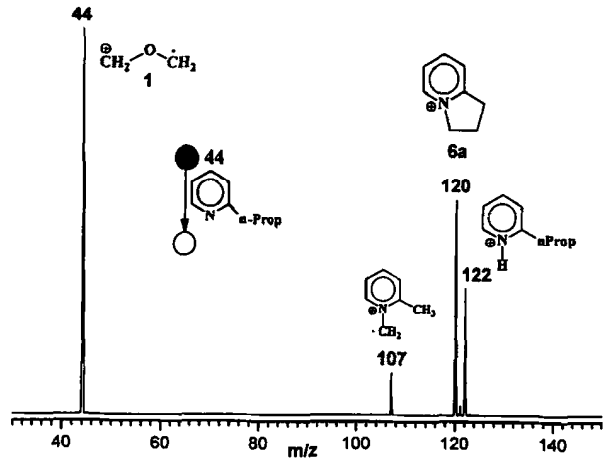

Figure 3. MS^2 product spectrum for ion–molecule reactions between the mass-selected ion **1** and 2-*n*-propyl pyridine that shows the surviving reactant ion (m/z 44), protonated 2-*n*-propyl pyridine (m/z 122), and fragments that correspond to $CH_3^{\cdot}$ (m/z 120) and C_2H_4 (m/z 107) loss from the unstable $CH_2^{+\cdot}$ transfer product.

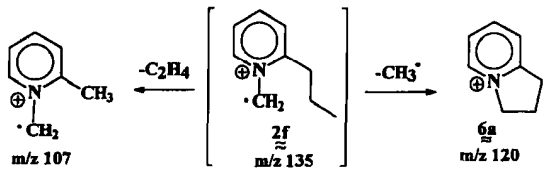

Scheme V

Reactions with Aromatic Five-Membered Heterocyclic Compounds

Similarly to the pyridine case, net $CH_2^{+\cdot}$ transfer from **1** to the heteroatom of furan, thiophene, pyrrole, and *N*-methyl pyrrole could lead to an interesting series of distonic ions **7** (Scheme VI). These ions are more likely to be formed for furan and thiophene, whose heteroatoms have an unshared electron pair other than that utilized in the formation of the aromatic sextet, and could therefore be capable of forming *O*- or *S*-methylene derivatives. Formation of ion **7b**, the ionized form of the simplest thiophene sulfur ylide, would parallel solution phase results that have shown the generation of stable sulfur ylides [17a] and *S*-methyl thiophenium cations [17b].

The ab initio calculations (Table 3) show, however, that contrary to pyridine (for which formation of the distonic radical cations **2a** was shown to be highly thermodynamically favorable), the most thermodynamically favorable process for these heterocyclic compounds is $CH_2^{+\cdot}$ transfer to the ring, not to the heteroatoms. This is so because the distonic ions **7a,c** are shown by calculation to be much less stable than the corresponding products of $CH_2^{+\cdot}$ transfer to the aromatic rings (**8a,c**) and thus, although this is only a thermodynamic preference, ring $CH_2^{+\cdot}$ transfer is more likely to prevail.

In accordance with a thermodynamically controlled process, the reactions of ion **1** with the five-membered heterocyclic compounds yield mainly CH^+, not $CH_2^{+\cdot}$, transfer products (Table 1), as exemplified for pyrrole in Figure 4. The CH^+ transfer products (m/z 80 in Figure 4) strongly point to reaction at the ring (Scheme VI) because the alternative product ions **7** would not be expected, by analogy with ion **2a** (Table 2), to fragment extensively by hydrogen atom loss. On the other hand, such fragmentation can be rationalized easily for ions **8**, a process that would yield the cations **9** (Scheme VI). Such ions (**9**) are known to be unstable [18] and to undergo rapid isomerization by ring-expansion to yield the aromatic six-membered heterocyclic cations **10** (Scheme VI), that is, the pyrilium (**10a**), thiapyrilium (**10b**), protonated pyridine (**10c**) and the *N*-methyl pyridinium cation (**10d**), respectively. Formation of the cations **10** are all evidenced by the great similarity observed when comparing their MS^3 spectra (Table 4) with the MS^2 CID product spectra of authentic ions, as exemplified for protonated pyridine (**10c**) in Figure 5a, b.

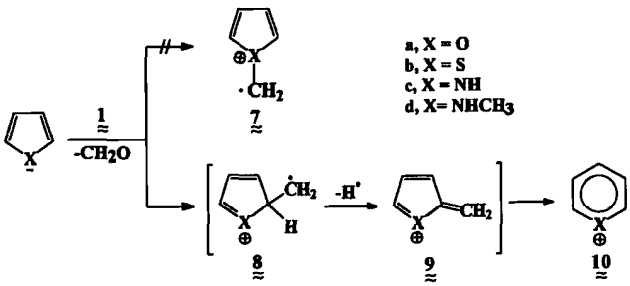

Scheme VI

Reactions with Saturated Heterocyclic Compounds

Ion **1** completely fails to transfer $CH_2^{+\cdot}$ to tetrahydrofuran (Table 1), and the corresponding MS^2 spectrum displays mainly protonated tetrahydrofuran (m/z 73) and a fragment at m/z 71 that corresponds to loss of a hydrogen atom from ionized tetrahydrofuran (m/z 72). On the other hand, the $CH_2^{+\cdot}$ transfer does occur for the sulfur analog tetrahydrothiophene, which yields a m/z 102 product to a moderate extent (Figure 6). The distonic *S*-methylene sulfonium ion **11** is the most likely product, because electrophilic attack should occur at the sulfur atom (Scheme VII). On the other hand, further isomerization to either ionized pentamethylene sulfide (**12**) or ionized methyl tetrahydrothiophene (**13**) may occur because the ab initio calculations (Table 3) show greater stabilities for the latter two ions. However, the MS^3 spectra of the m/z 102 product (Figure 7a) is very different from the MS^2 spectra of both the authentic ions **12** (Figure 7b) and **13** (Figure 7c), which strongly indicates formation of the sulfur distonic ion **11**. A comparison of these three spectra clearly shows that no or negligible isomerization of ion **11** has occurred. That α-sulfur distonic ions of the type $RRS^+—CH_2^{\cdot}$ are less thermodynamically stable than

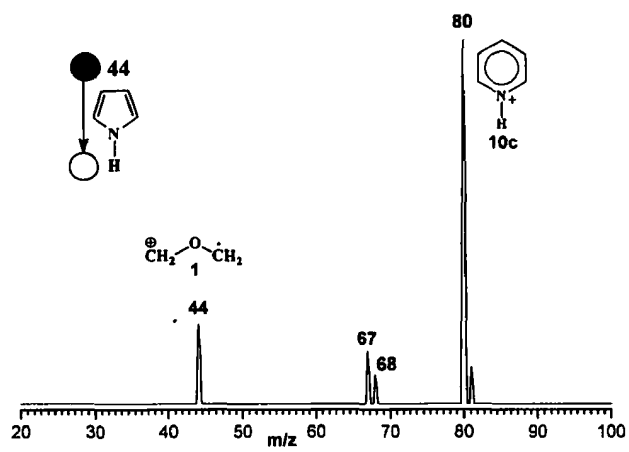

Figure 4. MS^2 product spectrum for ion–molecule reactions between the mass-selected ion **1** and pyrrole that shows the surviving reactant ion (m/z 44), protonated (m/z 68), and ionized pyrrole (m/z 67) and an abundant CH^+ addition product at m/z 80.

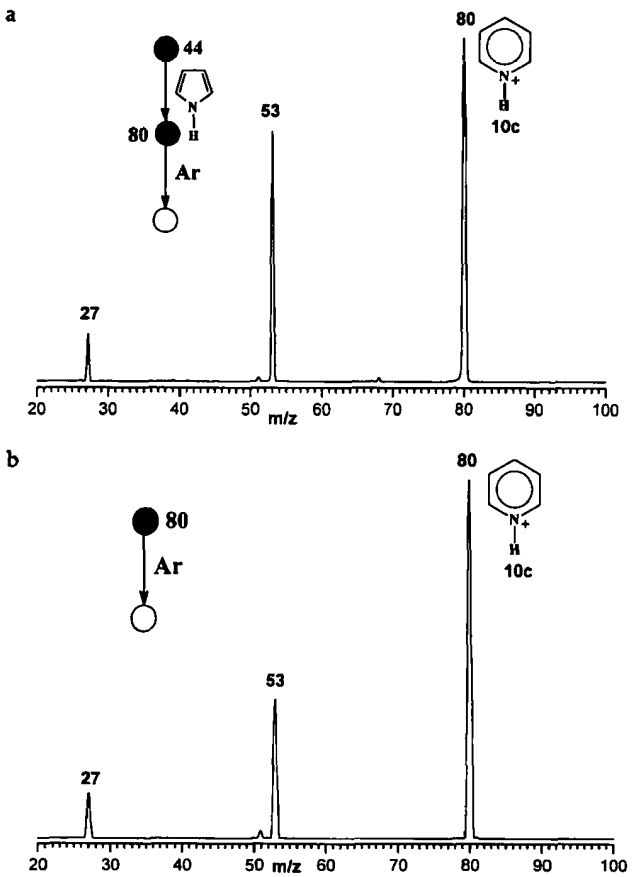

Figure 5. (a) MS^3 sequential product spectrum of the m/z 80 product formed in reactions between ion **1** and neutral pyrrole and (b) the MS^2 CID product spectrum of the authentic protonated pyridine. Both spectra show a practically identical CID fragmentation, which is indicative of similar structures.

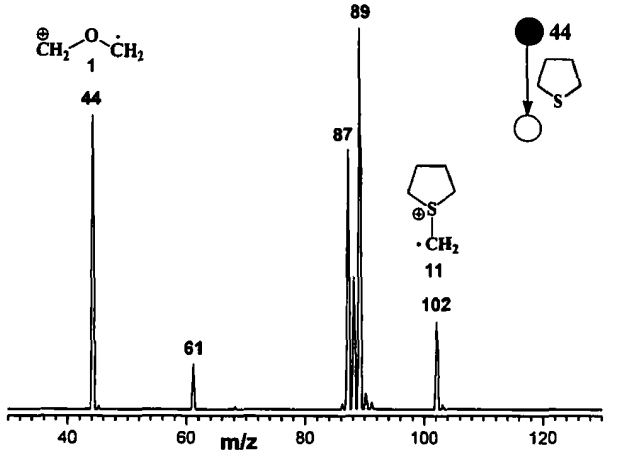

Figure 6. MS^2 product spectrum for ion–molecule reactions between mass-selected ion **1** and tetrahydrothiophene that shows the surviving reactant ion (m/z 44), protonated (m/z 89) and ionized (m/z 88) tetrahydrothiophene and its hydrogen atom loss fragment at m/z 87, and the $CH_2^{+\cdot}$ transfer product at m/z 102.

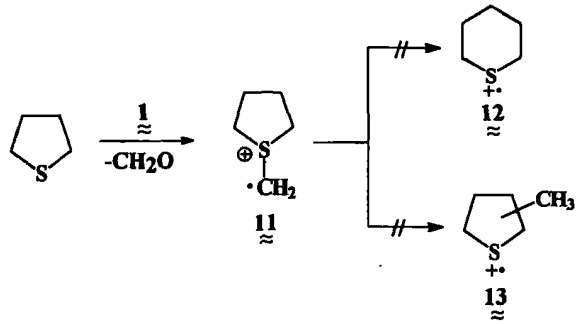

Scheme VII

their conventional isomers, but sufficiently kinetically stable toward isomerization in the gas phase, appears therefore to be a general trend. Kenttämaa and co-workers [19] also have recently shown by ab initio calculations that the distonic sulfur ion $CH_3S^+(CH_2^{\cdot})CH_3$ is less stable than its conventional isomer $CH_3CH_2SCH_3^{+\cdot}$, but the former is sufficiently stable in the gas phase so that its isolation and identification can be achieved.

The optimized structure with partial charge and spin densities of the new distonic sulfur radical cation **11** are presented in Figure 8, whereas all its angles and bond lengths can be obtained from the Cartesian coordinates presented in Table 5. Note the highly localized spin density (0.94) on the methylene carbon and the high positive charge (0.68) on the sulfur atom, which are characteristic of a distonic structure. Note also the tetrahedral sulfur atom, which bears an unshared electron pair.

The product spectra for reactions between ion **1** and the cyclic amines piperidine and pyrrolidine show formation of net CH^+ transfer products (Table 1). This reaction can therefore be rationalized to occur by initial transfer of $CH_2^{+\cdot}$ to the nitrogen to yield the distonic ions **14** as unstable intermediates, followed by their rapid α-NH hydrogen atom loss that yields the closed-shell immonium ions **15** (Scheme VIII). The CID MS^3 spectra of these immonium ions (**15a,b**) are show in Table 4.

Conclusions

By application of multiple stage mass spectrometric experiments performed in a pentaquadrupole instrument, the ion–molecule reactions between mass-selected ion **1** and several heterocyclic compounds could be investigated in detail. This was achieved by structural variations of the reactant molecules and the characterization of ionic products. The results also illustrate some applications of these reactions to the synthesis of ionic species and to distinction of isomeric neutral reagents. Ionized methylene transfer is the main reaction observed for a variety of pyridines and the *N*-methylene pyridinium distonic radical cations (**2a-f**) are formed as major products. Their *N*-methylene

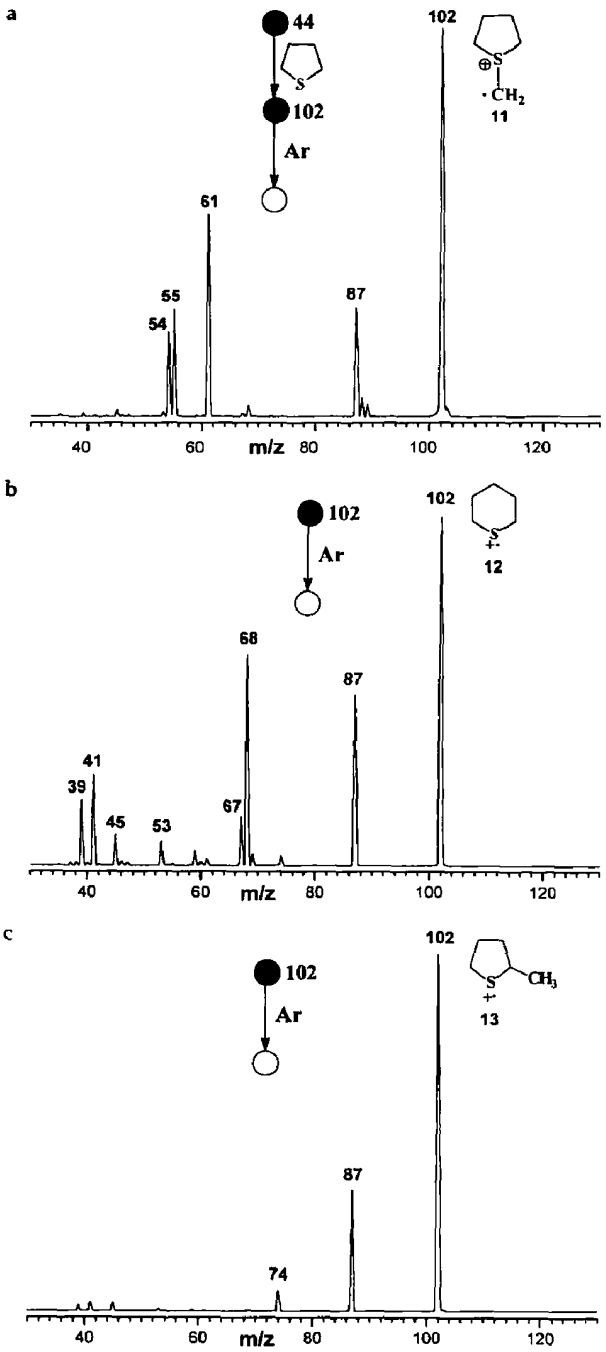

Figure 7. (a) MS^3 sequential product spectrum of the m/z 102 product ion formed in reactions between ion 1 and tetrahydrothiophene and the MS^2 CID product spectra of the authentic ions (b) 12 and (c) 13. The unique CID fragmentation displayed in (a) characterizes the sulfur distonic ion 11.

free-radical sites promote interesting ortho and para effects that greatly diversify the fragmentation patterns and thus allow easy distinction between them. This ion–molecule reaction can therefore be visualized as a useful approach to distinguish isomeric series of ring-substituted pyridines and derivatives.

The δ-cleavage process by which the ortho effect operates allows the synthesis of bicyclic pyridinium cations (6) when appropriate 2-substituted pyridines

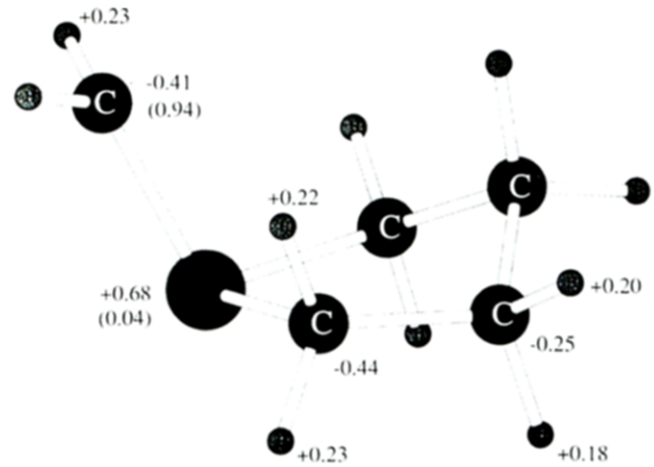

Figure 8. UHF/6-31G(d,p) optimized structure and some charge and spin densities (in parentheses) of the new distonic S-methylene sulfonium ion **11**. Similar values are obtained for nearly symmetrical atoms, for instance, the two methylene hydrogens, and are not shown.

are reacted with the distonic ion 1. The net CH^+ transfer from 1 consists of an interesting gas phase method for five- to six-membered ring expansion of aromatic heterocyclic compounds. In this study, formation of the pyrilium, thiapyrilium, protonated, and methylated pyridine cations (**10a–d**) have been demonstrated from furan, thiophene, pyrrole, and N-methyl pyrrole, respectively. Similar results are expected for their analogues and derivatives.

Reactions with tetrahydrothiophene lead to the synthesis of a new distonic S-methylene sulfonium ion **11**. This consists of another example of a sulfur distonic ion that is kinetically stable and does not isomerize to its more thermodynamically stable conventional radical cation isomers (**12** and **13**). The N-methylene distonic ions (**14**) formed by $CH_2^{+\cdot}$ transfer to the cyclic amines pyrrolidine and piperidine are likely to be

Table 5. Cartesian coordinates of the UHF/6-31G(d,p) optimized structure of the sulfur distonic ion **11**

S	−1.044101	−0.417263	−0.317662
C	−0.120532	−0.695043	1.257704
C	1.364736	−0.627432	0.874266
C	1.509253	0.408890	−0.240488
C	0.439845	0.080397	−1.283303
H	−0.432379	−1.649137	1.655112
H	−0.411469	0.095045	1.935391
H	1.700336	−1.599600	0.530345
H	1.948623	−0.369823	1.748758
H	2.489827	0.374238	−0.698555
H	1.357408	1.411247	0.145042
H	0.694650	−0.782632	−1.883277
H	0.164933	0.897295	−1.935391
O	−1.890456	1.100796	−0.041851
H	−2.489827	1.154166	0.847082
H	−2.175100	1.649137	−0.919724

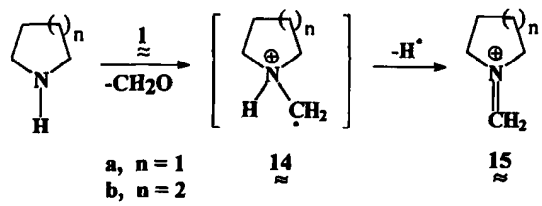

Scheme VIII.

unstable because of the presence of α-NH hydrogens, which makes available an energetically favorable fragmentation process that leads to closed-shell immonium cations (**15**).

Acknowledgments

The authors are greatly indebted to Dr. R. G. Cooks for invaluable discussions. This work was supported by the Research Support Foundation of the State of São Paulo (FAPESP) and the Brazilian National Research Council (CNPq).

References

1. (a) Yates, B. F.; Bouma, W. J.; Radom, L. *J. Am. Chem. Soc.* **1984**, *106*, 5805; (b) Yates, B. F.; Bouma, W. J.; Radom, L. *Tetrahedron* **1986**, *42*, 6225.
2. (a) Hammerum, S. *Mass Spectrom. Rev.* **1988**, *7*, 123; (b) Bouchoux, G. *Mass Spectrom. Rev.* **1988**, *7*, 203; (c) Stirk, K. M.; Kiminkinen, M.; Kenttämaa, H. I. *Chem. Rev.* **1992**, *92*, 1649; (d) Kenttämaa, H. I. *Org. Mass Spectrom.*, in press;
3. (a) Bouma, W. J.; MacLeod, J. K.; Radom, L. *J. Am. Chem. Soc.* **1980**, *102*, 2246; (b) Terlouw, J. K.; Heerma, W.; Dijkstra, G. *Org. Mass Spectrom.* **1981**, *16*, 326; (c) Bouma, W. J.; Nobes, R. H.; Radom, L. *J. Am. Chem. Soc.* **1983**, *105*, 1743; (d) Radom, L.; Bouma, W. J.; Nobes, R. H.; Yates, B. F. *Pure Appl. Chem.* **1984**, *56*, 1831; (e) Yates, B. F.; Bouma, W. J; Radom, L. *J. Am. Chem. Soc.* **1984**, *106*, 5805; (f) Yates, B. F.; Bouma, W. J; Radom, L. *Tetrahedron* **1986**, *22*, 6225; (g) Bouchoux, G. *Mass Spectrom. Rev.* **1988**, *7*, 203.
4. Bush, K. L.; Glish, G. L.; McLuckey, S. A. *Mass Spectrometry / Mass Spectrometry: Techniques and Applications of Tandem Mass Spectrometry*; VHC Publishers; New York, 1989.
5. (a) Staley, R. H.; Cordeman, R. R.; Foster, M. S.; Beauchamp, J. L. *J. Am. Chem. Soc.* **1974**, *96*, 1260; (b) Corderman, R. R.; Lebreton, P. R.; Buttrill, S. E.; Williamson, A. D.; Beauchamp, J. L. *J. Chem. Phys.* **1976**, *65*, 4929; (c) Bouma, W. J.; MacLeod, J. K.; Radom, L. *J. Chem. Soc. Chem. Commun.* **1978**, 724; (d) Bouma, W. J.; MacLeod, J. K.; Radom, L. *Adv. Mass. Spectrom.* **1979**, *8A*, 178; (e) de Koster, C. G.; van Houte, J. J.; Shadid, J. B.; van Thuijl, J. *Rapid Commun. Mass Spectrom.* **1988**, *2*, 97; (f) de Koster, C. G.; van Houte, J. J.; van Thuijl, J. *Int. J. Mass Spectrom. Ion Processes* **1990**, *98*, 235; (g) Rusli, R. D.; Schwarz, H. *Chem. Ber.* **1990**, *123*, 535; (h) Stirk, K. M.; Orlowski, J. C.; Leeck, D. T.; Kenttämaa, H. I. *J. Am. Chem. Soc.* **1992**, *114*, 8604; (i) Smith, R. L.; Franklin, R. L.; Stirk, K. M.; Kenttämaa, H. I. *J. Am. Chem. Soc.* **1993**, *115*, 10348; (j) Yu, S. J.; Gross, M. L.; Fountain, K. R. *J. Am. Soc. Mass Spectrom.* **1993**, *4*, 117.
6. (a) Baumann, B. C.; MacLeod, J. K. *J. Am. Chem. Soc.* **1981**, *103*, 6223; (b) Van Velzen, P. N. T.; Van der Hart, W. *J. Chem. Phys. Lett.* **1981**, *83*, 56; (c) Bally, T.; Nitsche, S.; Haselbach, E. *Helv. Chim. Acta* **1984**, *67*, 86; (d) Qin, X. Z.; Snow, L. D.; Williams, F. *J. Am. Chem. Soc.* **1985**, *107*, 3366; (e) Bouma, W. J.; Poppinger, D.; Saebo, S.; MacLeod, J. K.; Radom, L. *Chem. Phys. Lett.* **1984**, *104*, 198; (f) Mabud, Md. A.; Ast, T.; Verma, S.; Jiang, Y.-X.; Cooks, R. G. *J. Am. Chem. Soc.* **1987**, *109*, 7597; (g) Wesdemiotis, C.; Leyh, B.; Fura, A.; McLafferty, F. W. *J. Am. Chem. Soc.* **1990**, *112*, 8655.
7. (a) Eberlin, M. N. *Proceedings of the 41st ASMS Conference on Mass Spectrometry and Allied Topics*, 1993; p 975; (b) Gozzo, F. C.; Eberlin, M. N., to appear.
8. (a) Shay, B. J.; Eberlin, M. N.; Cooks, R. G.; Wesdemiotis, C. *J. Am. Soc. Mass Spectrom.* **1992**, *3*, 518; (b) Kotiaho, T.; Shay, B. J.; Cooks, R. G.; Eberlin, M. N. *J. Am. Chem. Soc.* **1993**, *115*, 1004; (c) Eberlin, M. N.; Majumdar, T. K.; Cooks, R. G *J. Am. Chem. Soc.* **1992**, *114*, 2884; (d) Eberlin, M. N.; Cooks, R. G *J. Am. Chem. Soc.* **1993**, *115*, 9226; (e) Eberlin, M. N.; Cooks, R. G. *Org. Mass Spectrom.* **1993**, *28*, 679; (f) Eberlin, M. N.; Kotiaho, T.; Shay, B.; Yang, S. S.; Cooks, R. G, *J. Am. Chem. Soc.* **1994**, *116*, 2457; (g) Bortolini, O.; Yang, S. S.; Cooks, R. G. *Org. Mass Spectrom.* **1993**, *28*, 1313; (h) Eberlin, M. N.; Morgon, N. H.; Yang, S. S.; Shay, B. J.; Cooks, R. G. *J. Am. Soc. Mass Spectrom.* **1995**, *6*, 1.
9. (a) Schwartz, J. C.; Schey, K. L.; Cooks, R. G *Int. J. Mass Spectrom. Ion Processes* **1990**, *101*, 1; (b) Juliano, V. F.; Kascheres, C.; Eberlin, M. N.; Lago, C. L., to appear.
10. (a) Hanús, V.; Cermáck, V. *Collect. Czech. Chem. Commun.* **1959**, *24*, 1602; (b) Spilker, R.; Grutzmacher, H. F. *Org. Mass Spectrom.* **1986**, *21*, 459.
11. Gaussian92, revision C, Frisch, M. J.; Trucks, G. W.; Head-Gordon, M.; Gill, P. M. W.; Wong, M. W.; Foresman, J. B.; Johnson, B. G.; Schlegel, H. B.; Robb, M. A.; Replogle, E. S.; Gomperts, R.; Andres, J. L.; Raghavachari, K.; Binkley, J. S.; Gonzales, C.; Martin, R. L.; Fox, D. J.; Defrees, D. J.; Baker, J.; Stewart, J. J. P.; Pople, J. A., Gaussian, Inc., Pittsburgh PA, 1992.
12. (a) Hehre, W. J.; Ditchfield, R.; Pople, J. A. *J. Chem. Phys.* **1972**, *56*, 2257; (b) Hariharan, P. C.; Pople, J. A. *Theor. Chem. Acta* **1973**, *72*, 650; (c) Gordon, M. S. *Chem. Phys. Lett.* **1980**, *76*, 163; (d) Frisch, M. J.; Pople, J. A.; Binkley, J. S.; *J. Chem. Phys.* **1984**, *80*, 3265.
13. Møller, C.; Plesset, M. S. *Phys. Rev.* **1934**, *46*, 618.
14. Xmol, version 1.3.1, Minnesota Supercomputer Center, Inc., Minneapolis, MN, 1993.
15. Yu, S. J.; Holliman, C. L.; Rempel, D. L.; Gross, M. L. *J. Am. Chem. Soc.* **1993**, *115*, 9676.
16. Cooks, R. G.; McDonald, R. N.; Cranor, P. T.; Petty, H. E.; Wolfe, N. L. *J. Org. Chem.* **1973**, *38*, 1114.
17. (a) Porter, A. E. *Adv. Heterocyclic Chem.* **1989**, *45*, 151; (b) Brumlik, G. C.; Kosak, A. L.; Pitcher, R. *J. Am. Chem. Soc.* **1964**, *86*, 5360.
18. Health, T. G.; Allison, J.; Watson, J. T. *J. Am. Chem. Soc.* **1991**, *2*, 270.
19. Smith, R. L.; Chyall, L. J.; Stirk, K. M.; Kenttämaa, H. I. *Org. Mass Spectrom.* **1993**, *28*, 1623.